Assimilation of IRS-P4 (MSMR) meteorological data in the NCMRWF global data assimilation system

Rupa Kamineni*, S R H Rizvi, S C Kar, U C Mohanty* and R K Paliwal

National Centre for Medium Range Weather Forecasting (NCMRWF), Mausam Bhavan, Lodi Road, New Delhi 110 003, India.

**Centre for Atmospheric Sciences, I.I.T., New Delhi 110 016, India.*

Oceansat-1 was successfully launched by India in 1999, with two payloads, namely Multi-frequency Scanning Microwave Radiometer (MSMR) and Ocean Color Monitor (OCM) to study the biological and physical parameters of the ocean. The MSMR sensor is configured as an eight-channel radiometer using four frequencies with dual polarization. The MSMR data at 75 km resolution from the Oceansat-I have been assimilated in the National Centre for Medium Range Weather Forecasting (NCMRWF) data assimilation forecast system. The operational analysis and forecast system at NCMRWF is based on a T80L18 global spectral model and Spectral Statistical Interpolation (SSI) scheme for data analysis. The impact of the MSMR data is seen globally, however it is significant over the oceanic region where conventional data are rare. The dry-nature of the control analyses have been removed by utilizing the MSMR data. Therefore, the total precipitable water data from MSMR has been identified as a very crucial parameter in this study. The impact of surface wind speed from MSMR is to increase easterlies over the tropical Indian Ocean. Shifting of the positions of westerly troughs and ridges in the south Indian Ocean has contributed to reduction of temperature to around 30°S.

1. Introduction

Numerical weather prediction (NWP), sea state forecast as well as the study of climate variations require a complete and accurate description of the initial state of the atmosphere and ocean. Unfortunately, no single component of the observing system measures the atmosphere and ocean with sufficient accuracy and completeness. Conventional global observations taken at synoptic hour is not sufficient to resolve the atmospheric state at any point of time, asynoptic observations from other sources like satellite, radar etc. must be incorporated for accurately prescribing the initial state of the atmosphere. The field of satellite has made rapid advances and today, there are a host of space missions providing data on various parameters such as surface winds, cloud liquid water, total precipitable water content, rain rate, SST, ozone concentration etc. Space observations provide asynoptic and repetivity coverage of the ocean in contrast to the sparse and isolated *in situ* observations. Spaceborne sensors provide observations over the ocean, which are inaccessible to ships. Satellite observations of oceanic variables provide critical fields for the study of the earth's climate system, calibration of climate models, general circulation models etc. Also various types of satellite observations, both from polar as well as geo-stationary satellites have been generating at different resolutions as low as 10 km. Currently under various satellite programs, different types of global data are available from TOVS, TRMM, SSM/I etc. almost on real time basis.

Satellite microwave radiometers have been successfully used to monitor the temporal and spatial variations of sea surface and atmospheric properties on a global scale. This includes the

Keywords. MSMR data; wind speed; total precipitable water content; GDAS; impact.

Proc. Indian Acad. Sci. (Earth Planet. Sci.), **111**, No. 3, September 2002, pp. 351–364

validation of microwave radiometer geophysical parameters using meteorological model analysis (Eymard *et al* 1993), comparative studies (Varma *et al* 1998), rainfall, cloud liquid water, surface winds and precipitation related studies (Schluessel and Emery 1990; Schluessel and Luthardt 1991; Chang and Holt 1994; Ledvina and Pfaendtner 1995; Weng *et al* 1997; Xiao *et al* 2000 etc.).

Oceansat-1 was successfully launched by India in 1999, with two payloads, namely Multi-frequency Scanning Microwave Radiometer (MSMR) and Ocean Color Monitor (OCM) to study the biological and physical parameters of the ocean. The MSMR sensor is configured as an eight-channel radiometer using four frequencies with dual polarization. The main geo-physical parameters derived at three different resolutions (150, 75 and 50 km) are sea surface temperature, surface wind speed, total precipitable water content and cloud liquid water. In Rizvi *et al* (2000) and Rizvi *et al* (2002), we have described the impact of MSMR data at 150 km resolution on the data assimilation system. Recently, wind speed and total precipitable water data from SSM/I sensor on board DMSP satellite are being assimilated in the operational data assimilation system of NCMRWF. We have also carried out assimilation experiments using TRMM (TMI) wind speed and water vapor data. Results of these parallel assimilation experiments and comparison with MSMR data will be presented elsewhere. Rizvi *et al* (2002) have carried out assimilation experiments with MSMR data at 150 km resolution. Since then, reprocessed MSMR data at 75 km resolution was made available to us. It may be noted that both TMI and SSM/I data are available at 25 km resolution. Therefore, it was of interest to know the impact of the newly available MSMR data at a finer resolution (i.e. 75 km) in the data assimilation system. This study also shows the positive aspects of the MSMR data obtained from the Indian satellite and will prove very useful for the utilization of the data from microwave sensors from future Indian satellites. Goswami and Rajagopal (2002) have compared the NCMRWF analyzed fields against other satellite products and NCEP re-analyses and found that the NCMRWF analyses improved when SSM/I data were assimilated.

MSMR surface wind speed and total precipitable water content data, derived at 75 km resolution, is assimilated along with global meteorological data, received through RTH, New Delhi in the NCMRWF Global Data Assimilation System. Section 2 briefly describes the global data assimilation system operational at NCMRWF. Various experiments are conducted to assess the impact of these parameters individually and together. The design of experiments is described in section 3. Results are discussed in section 4. The study is concluded in section 5.

2. NCMRWF Global data assimilation system

The operational analysis and the forecast suite at NCMRWF is based on a T80L18 global spectral model and Spectral Statistical Interpolation (SSI) scheme for data analysis, which are originally adapted from NCEP, USA. The model and analysis packages have undergone several modifications at NCMRWF. The analysis scheme is mainly based on the Lorenc (1986) concept of minimizing a cost function in terms of the deviation of desired analysis from the first guess field, which is taken as the six hour forecast, and the observations, weighted by the inverse of the forecast and observation errors respectively. An objective function (J) used for the SSI scheme is given by

$$J = 1/2(x - x_b)^T B^{-1}(x - x_b) + [y_{\text{obs}} - R(x)]^T O^{-1}[y_{\text{obs}} - R(x)], \quad (1)$$

where:

- x – N component vector of analysis variables.
- x_b – N component vector of background variables (also known as first guess).
- y_{obs} – M component vector of observations.
- B – M × N forecast-error covariance matrix.
- O – M × M observational error covariance matrix (including representative error).
- R – Transformation operator (possibly non-linear) that converts the analysis variables to the observation type and location.
- N – Number of degrees of freedom in the analysis.
- M – Number of observations.

The two terms in J on the right hand side of equation (1) deals with the fit of the first guess field and the observations with the analysis respectively. In order that the analysis should fit best with both the first guess and the observations, J should be minimized with respect to analysis variable x. In SSI, the minimization is accomplished using a descent algorithm, which allows R to be non-linear.

The analysis variables used in SSI are the sigma spectral coefficients of the amplitude of empirical orthogonal functions (EOFs) for vorticity (ζ), fast or unbalanced part of the divergence (D'), unbalanced temperature (T'), unbalanced log of surface

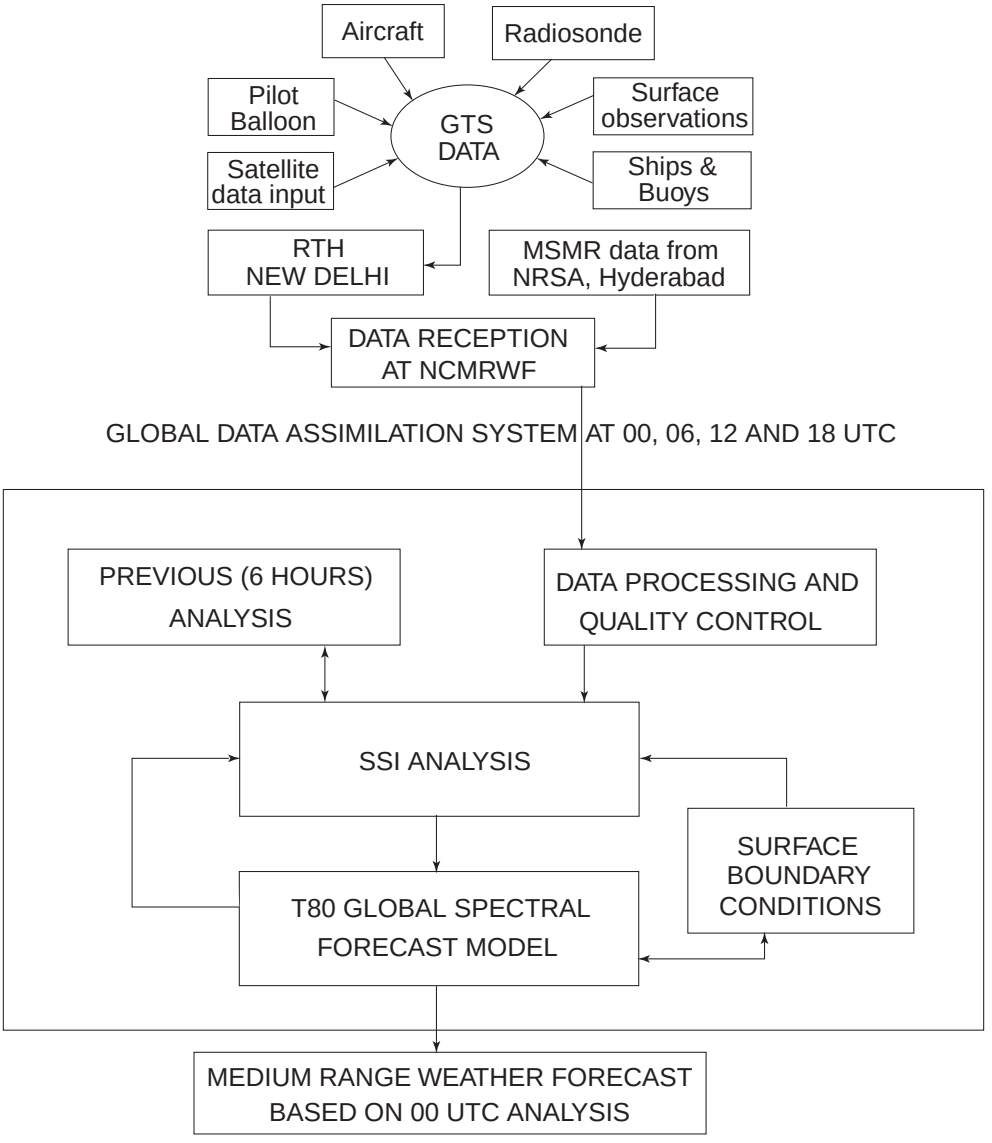

Figure 1. Flow chart of NCMRWF analysis/forecast system.

pressure ($\ln P'_s$), and mixing ratio (q). The distinction of balanced and unbalanced variables is a way of implicitly including a linear balance relationship. In SSI, an explicit refinement of this balance relationship is obtained by adding an additional constraint to the analysis objective function in which the full divergence tendency is adjusted to be close to the guess divergence tendency. This is treated in this way, as if divergence tendency were observed. The details about the choice of the analysis variables, balance between the mass and the wind field, vertical coupling and the statistical parameters used etc. are described in Parrish and Derber (1992) and Rizvi and Parrish (1995). The procedure for including wind speed and total precipitable water content are presented in Rizvi *et al* (2000), and Rizvi *et al* (2002). The schematic diagram showing different components of NCMRWF analysis/forecast system is given in figure 1.

The forecast model has a horizontal resolution of 80 waves with triangular truncation and 18 layers in the vertical (T80L18). The details of the model are documented in Kanamitsu (1989). The model has comprehensive physics packages for boundary layer, radiation and surface processes and convection. The analysis-forecast system is operational at NCMRWF since 1994. A brief description of the T80 Global spectral model is given in table 1.

3. Design of experiments

To evaluate the impact of MSMR wind speed and total precipitable water content data, four sets of experiments were performed with MSMR data along with global GTS data.

Table 1. *Brief description of global spectral model.*

Model elements	Components	Specifications
Grid	Horizontal	Global spectral-T80 (256 × 128).
	Vertical	18 Sigma layers [s = .995, .981, .960, .920, .856, .777, .688, .594, .497, .425, .375, .325, .275, .225, .175, .124, .074, .021].
	Topography	Mean.
Dynamics	Prognostic variables	Rel. vorticity, divergence, virtual temp., log (surface pressure), water vapour mixing ratio.
	Horizontal transform	Orszag's technique.
	Vertical differencing	Arakawa's energy conserving scheme.
	Time differencing	Semi-implicit with 900 seconds of time step.
	Time filtering	Robert's method.
	Horizontal diffusion	Second order over quasi-pressure surfaces, scale selective.
Physics	Surface fluxes	Monin - Obukhov similarity.
	Turbulent diffusion	K-Theory.
	Radiation	Short wave – Lacis & Hansen.
		Long wave – Fels and Schwarzkopf.
	Deep convection	Kuo scheme modified.
	Shallow convection	Tiedtke method.
	Large scale condensation	Manabe-modified scheme based on saturation.
	Cloud generation	Slingo scheme.
	Rainfall evaporation	Kessler's scheme.
	Land surface processes	Pan scheme having 3-layer soil model for soil temperature and bucket hydrology of Manabe for soil moisture prediction.
	Air-sea interaction	Roughness length over sea computed by Charnock's relation. Climatological SST, bulk formulae for sensible and latent heat fluxes.
	Gravity wave drag	Lindzen and Pierrehumbert Scheme.

- Control run (CNTR): In this experiment no MSMR-data were used and the assimilation cycle was run only with operationally available global GTS data.
- Experiment 1 (Exp. 1): In this experiment, the assimilation cycle was run with only MSMR-wind speed (WS) data together with all the global data used in CNTR.
- Experiment 2 (Exp. 2): In this experiment, the assimilation cycle was run with only MSMR-total precipitable water content (TPWC) data together with all the global data used in CNTR.
- Experiment 3 (Exp. 3): In this experiment, the assimilation cycle was run with both MSMR-wind speed and the total precipitable water content data together with all the global data used in CNTR.

In this paper, we have also made a brief comparison of analyses made using 75 km MSMR data with the analyzed data using 150 km resolution MSMR data described in Rizvi *et al* (2002).

4. Results and discussion

One of the data-sparse regions, the Indian Ocean basin (Arabian Sea, Bay of Bengal and Equatorial Indian Ocean) is selected for the impact study. Over this ocean, *in situ* observations are available rarely, so the only source of observations is from the satellite. Atmospheric condition over the Indian seas (Bay of Bengal and Arabian Sea) is also unique as the winds over this basin reverse semiannually, blowing from the southwest during southwest summer monsoon and from the northeast during the northeast winter monsoon. In the absence of any observed data over the oceanic region, the six-hour model forecast (serves as a background field and hereafter referred as Guess) is retained as the analysis. The behavior of the Guess, which has coarse resolution, is studied using the high-resolution MSMR data. To examine the impact of MSMR data, mean analysis and Guess for the period of 1st July to 15th July 1999 have been used. All the results presented in this paper are based on the

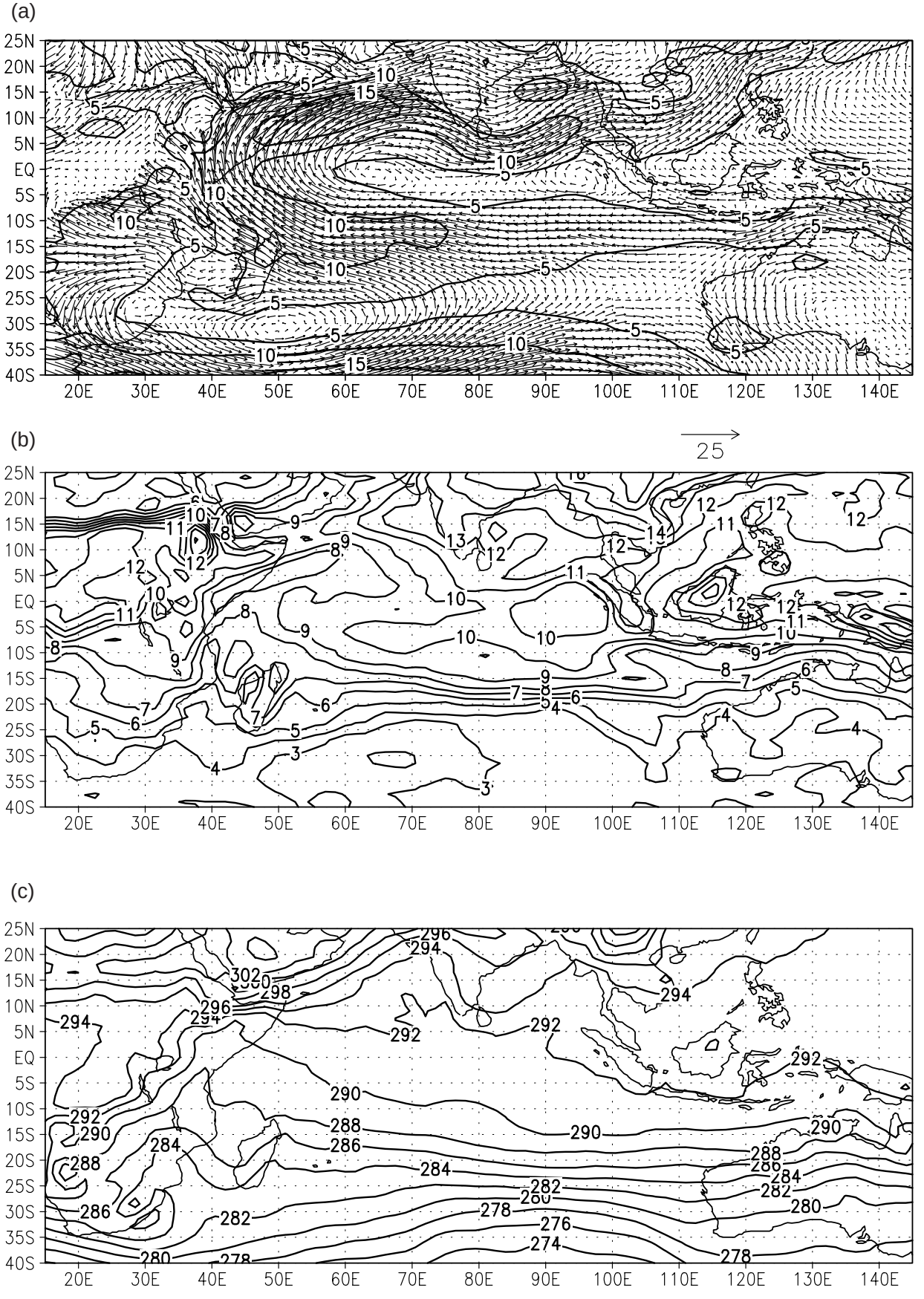

Figure 2. Mean CNTR analysis (July 1st –15th, 1999) of **(a)** wind (unit: m/s, contour interval: 5 m/s), **(b)** specific humidity (unit: gm/kg, contour interval: 1 gm/kg) and **(c)** temperature (unit: K, contour interval: 2°K) at 850 hPa.

mean analyzed fields for the period July 1st–15th, 1999.

The mean CNTR analysis of wind, specific humidity and temperature fields at 850 hPa are shown in figure 2. The distribution of mean wind field at 850 hPa shows the existence of strong Southern Hemispheric trades having a speed of about 10 m/s, strong cross equatorial flow into the Northern Hemisphere off the Somali coast and a strong zone of westerlies over the Arabian Sea (15–20 m/s) and the Bay of Bengal (10–15 m/s). The pattern of specific humidity and temperature fields broadly agrees with climatological features. Specific humidity is about 10 gm/kg around the equatorial belt. Over the Indian monsoon domain, the values of specific humidity are higher than those over the equatorial oceanic region. Figure 3 shows the differences of mean analyses of winds at 850 hPa of the MSMR experiments from that of CNTR. Exp. 1-CNTR (figure 3a) shows that the wind over ocean part has strengthened by 1 m/s. Especially the winds in the equatorial belt has strengthened by 2 m/s. The strengthening of Somali jet and the westerlies over the Arabian Sea and the Bay of Bengal is also noticed. Exp. 2-CNTR (figure 3b) shows the strengthening of Southern Hemispheric trades. This shows that the additional moisture data have influenced the wind field to some extent. Exp. 3-CNTR (figure 3c) shows that when both the data sets are used together, the impact has been enhanced. All winds over this region are strengthened by 1–2 m/s. The same type of features are noticed in the case of Guess also (figure not shown).

Different panels of figure 4 show the mean analysis of specific humidity differences with control run at 850 hPa. Exp. 1-CNTR (a) shows that there are slight changes over the ocean by about 0.5 gm/kg. That means the moisture field is influenced by the additional wind speed data. Exp. 2-CNTR (b) shows the increase of specific humidity over the entire ocean part, especially over the equatorial belt by about 1.5 gm/kg. Exp. 3-CNTR (c) shows a large increase over the equatorial belt (1–2 gm/kg) and other parts also by about 1 gm/kg. With the additional MSMR data, the wind and moisture fields strengthen around the equatorial belt. Elsewhere, the strengthening is noticed as isolated pockets. Same features are also observed in case of the background field (figure not shown). It may be noted that the operational analyses in 1999 are drier compared to most of the analyses from other NWP centers. Rizvi *et al* (2000), while analyzing the results of inclusion of MSMR data at 150 km had also noted this feature. Currently, SSM/I precipitable water data are being used in the operational analysis at NCMRWF, and the dry bias of the analyses has been removed. The mean differences of temperature analyses at 850 hPa with CNTR are shown in figure 5. First panel shows that Exp. 1 is cooler than CNTR analysis by about 1 degree over most parts of south Indian Ocean. This cooling is noticed to the south of 20°S. Slight warming is observed to the north of 20°S. Middle panel shows that Exp. 2 is warmer than CNTR by about 0.2°. This warming is noticed in the entire oceanic region. That means additional wind speed data contributed cooling and additional total precipitable water content data contributed to the warming. In case of Guess also, cooling is noticed by about 0.4°, when both the data sets are used together (figure not shown).

Figure 6 shows the zonal average difference of wind speed and specific humidity at 850 hPa. Wind field has strengthened more over Southern Hemisphere and tropics in Exp. 1 and Exp. 3, in which experiments MSMR wind speed data are used. In case of moisture, tropics and Northern Hemisphere are more moist than CNTR in Exp. 2 and Exp. 3, in which MSMR total precipitable water content data are used. This shows that by and large the impact of MSMR data is seen over tropics. Figure 7 shows the sectorial mean (45°E–100°E) pressure-latitude cross-section of specific humidity differences with the CNTR. Remarkable changes are noticed along the equator and in Southern Hemisphere. All MSMR experiments are more moist than CNTR. The differences of Exp. 1 with CNTR are about 0.2 gm/kg along the equator and 0.1 gm/kg in the Southern Hemisphere. There is no change to the south of 45°S and in Northern Hemisphere. These changes are noticed up to 550 hPa. In Exp. 2 and Exp. 3, the differences are up to 1 gm/kg in the equatorial region and these changes are maintained up to 400 hPa. Maximum difference is at 850 hPa. Over Southern Hemisphere, the differences are of the order of 0.5 gm/kg. There are small changes in the lower troposphere over the Northern Hemisphere. Dryness is observed at 10°S in the middle troposphere. So the MSMR total precipitable water content data has influenced the moisture filled at almost all the levels over Southern Hemisphere and the MSMR wind speed data also to some extent. Figure 8 shows the vertical cross-section of temperature differences with control run, mean for the sector (45°E–100°E). The temperature changes are noticed only in the Southern Hemisphere. In Exp. 1 and Exp. 3, there is a cooling in the belt of 20°S–40°S of the order of 0.7° and 0.5° respectively. This cooling is extended up to 400 hPa. In the upper troposphere also there is cooling around 30°S. Exp. 2 is warmer than CNTR up to 750 hPa. Above 750 hPa, there is cooling over 30°S–40°S belt. Some of the cooling seen in Exp. 1 is reduced due to inclusion of TPWC data in Exp. 3. It may

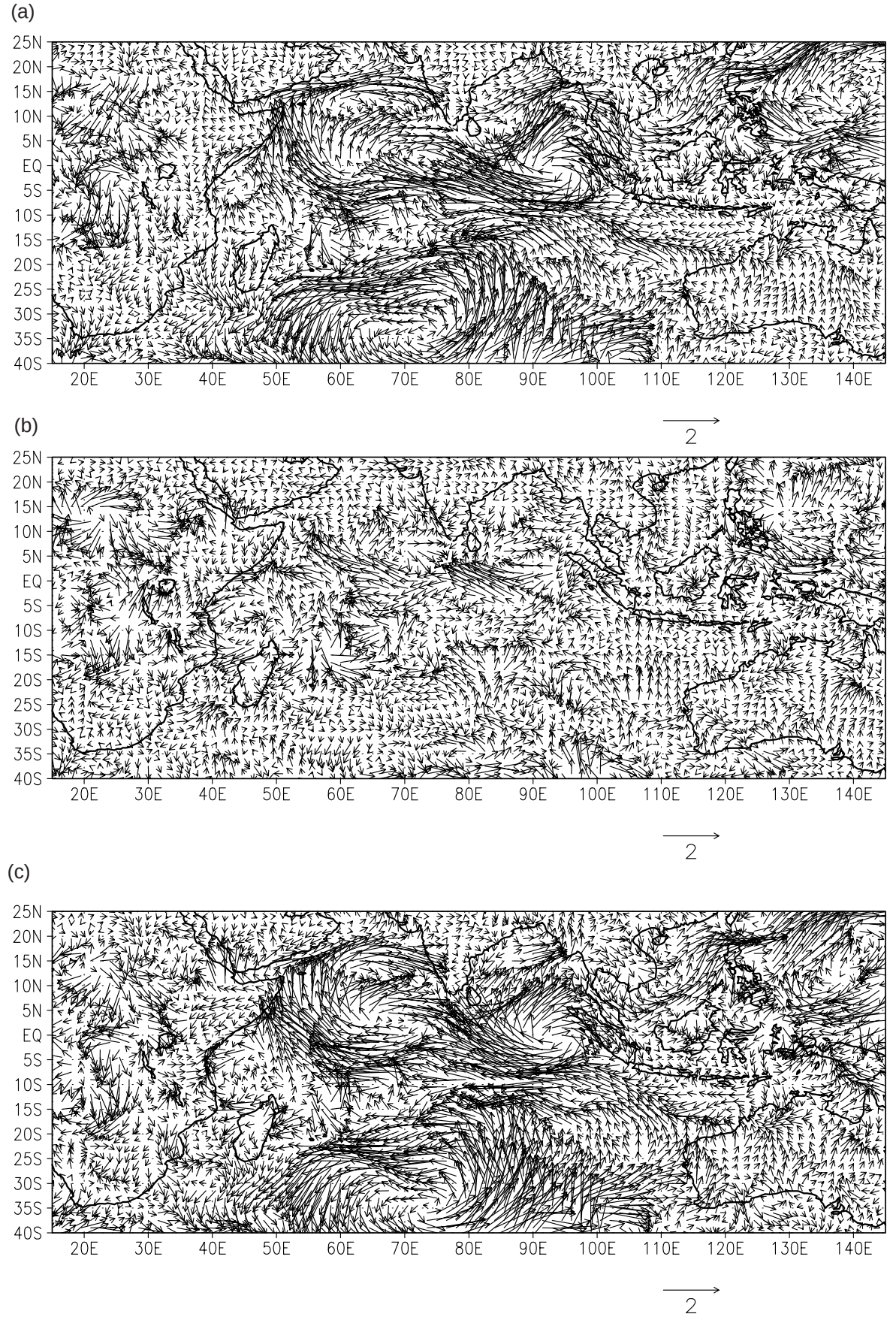

Figure 3. Mean analysis (July 1st –15th, 1999) of wind (m/s): **(a)** Exp. 1 – CNTR, **(b)** Exp. 2 – CNTR and **(c)** Exp. 3 – CNTR at 850 hPa.

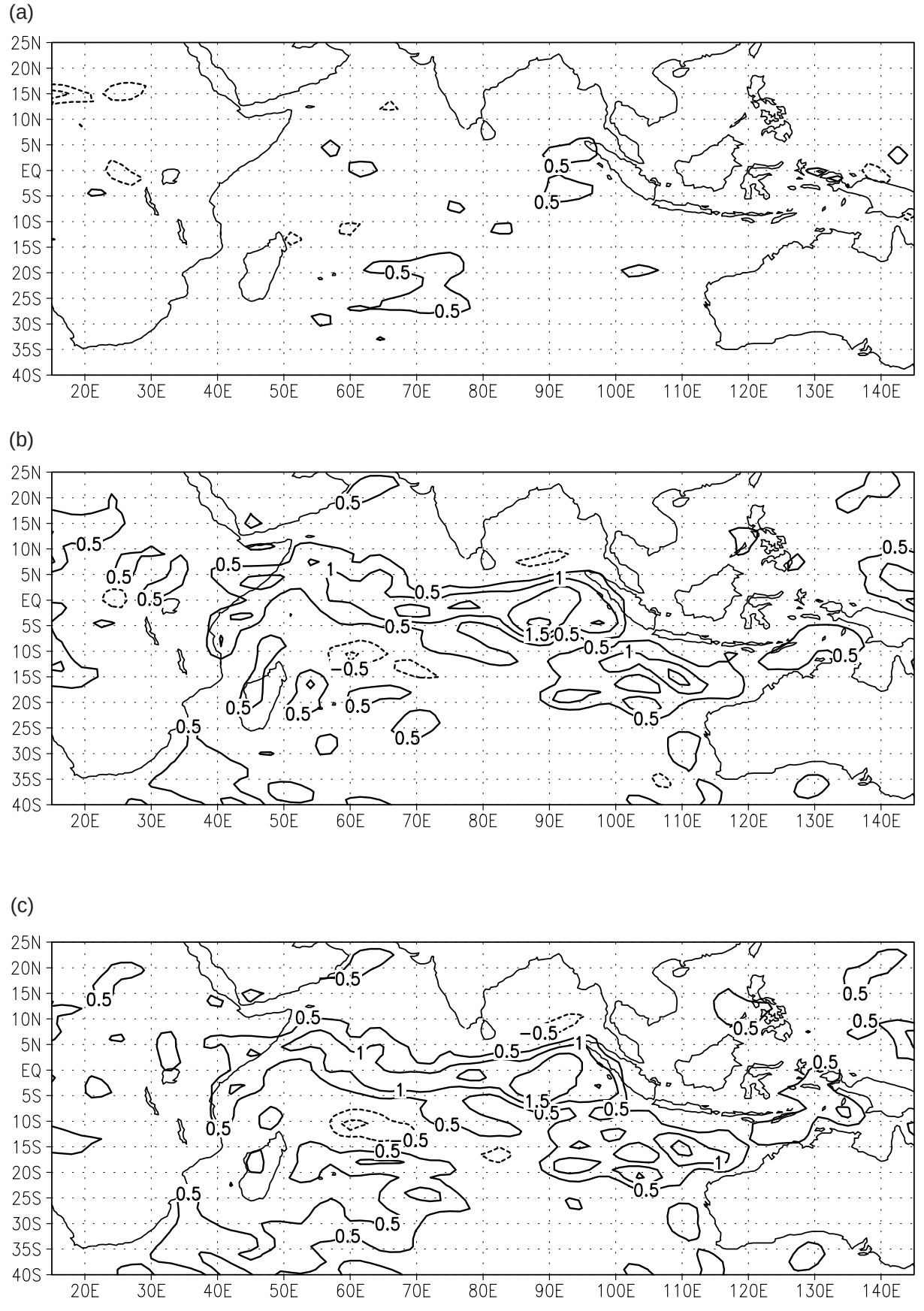

Figure 4. Mean analysis (July 1st –15th, 1999) of specific humidity: **(a)** Exp. 1 – CNTR, **(b)** Exp. 2 – CNTR and **(c)** Exp. 3 – CNTR at 850 hPa (unit: gm/kg, contour interval: 0.5 gm/kg).

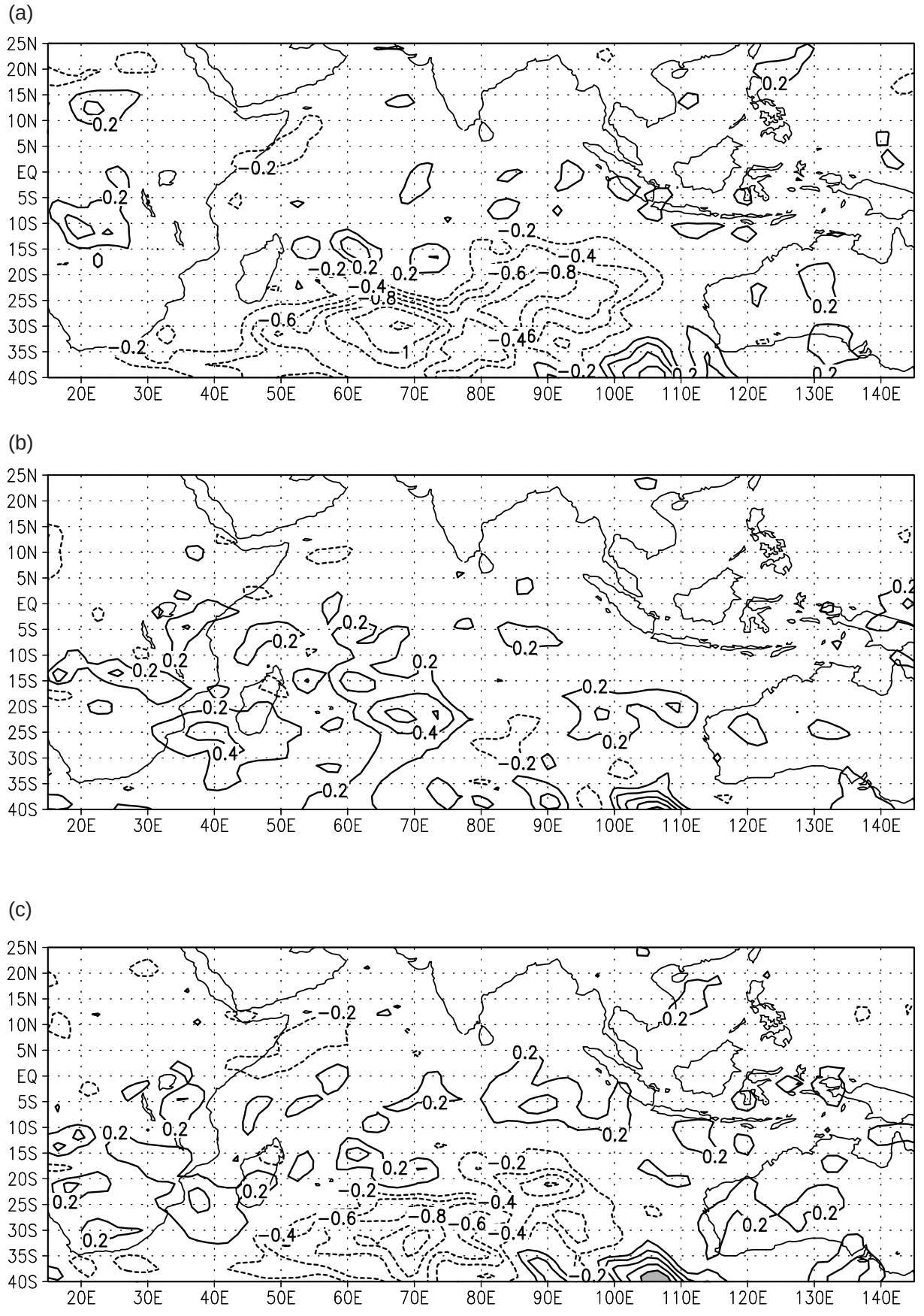

Figure 5. Mean analysis (July 1st –15th, 1999) of temperature: **(a)** Exp. 1 – CNTR, **(b)** Exp. 2 – CNTR and **(c)** Exp. 3 – CNTR at 850 hPa (unit: °K, contour interval: 0.2°K).

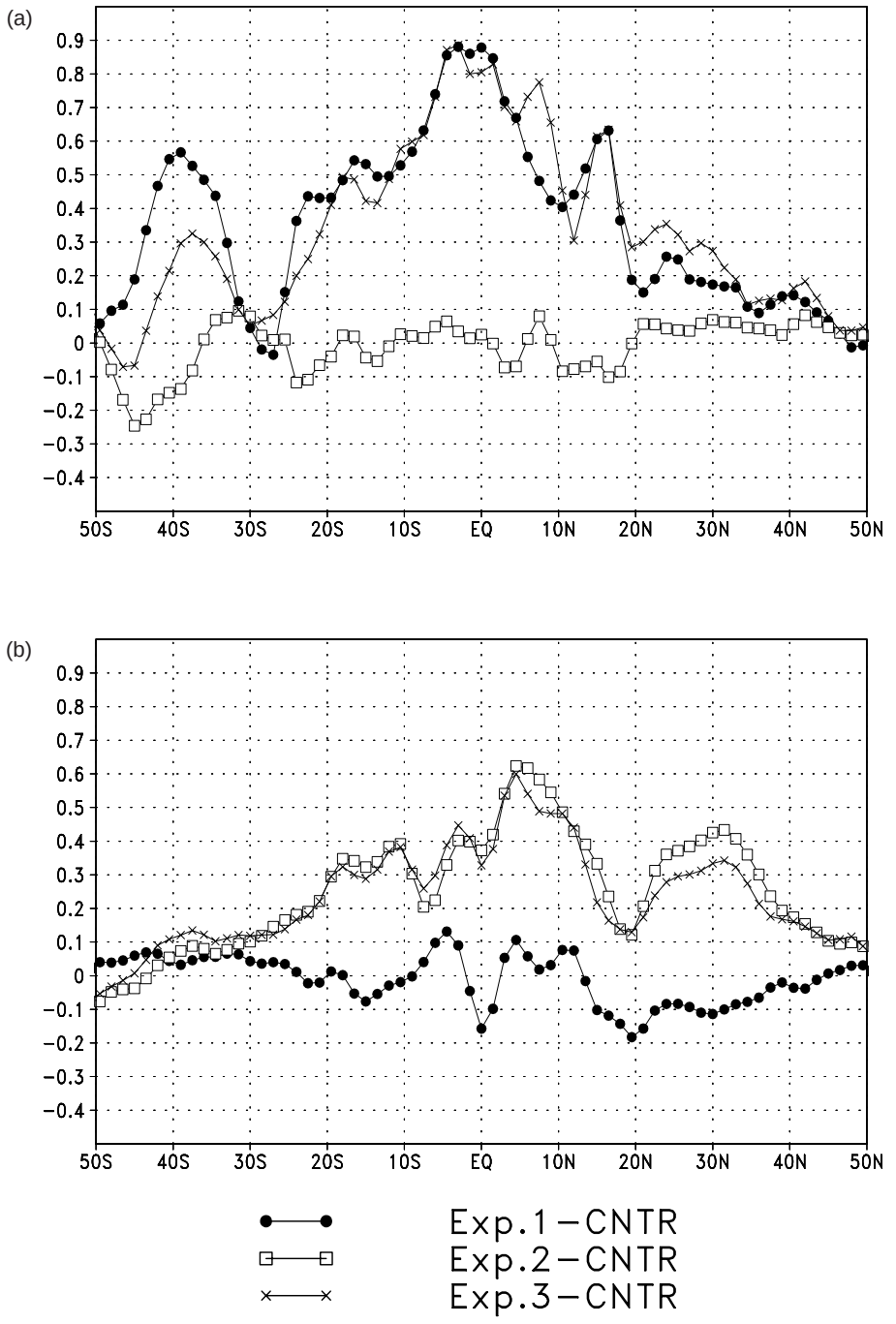

Figure 6. Zonal average difference (mean of July 1st–15th, 1999) of **(a)** wind speed (m/s) and **(b)** specific humidity (gm/kg) at 850 hPa for Exp. 1 – CNTR, Exp. 2 – CNTR and Exp. 3 – CNTR.

be noted that the positions of westerly troughs and ridges in the south Indian Ocean have changed by using MSMR wind data. Therefore, the temperature pattern has also changed considerably. This pattern may be due to the fact that only 15 days analyses have been used in this study. However, it may be noted that while using 150 km MSMR data Rizvi *et al* (2000) have also found similar features.

In figure 9, we show the mean analyses of wind at 850 hPa using MSMR data at 150 km. resolution for the same period (July 1st–July 15th). The difference of wind analyses obtained from 150 km and 75 km (corresponding to Exp. 3) are also shown in the figure (lower panel). The easterlies in the equatorial Indian Ocean are stronger with 75 km data. The monsoon winds in this case are also stronger. Specific humidity difference shows that in the Indian Ocean, 75 km data provides more moisture than the 150 km data (over equatorial eastern Indian Ocean). Circulation pattern over that region shows maximum difference between these two experiments. The differences

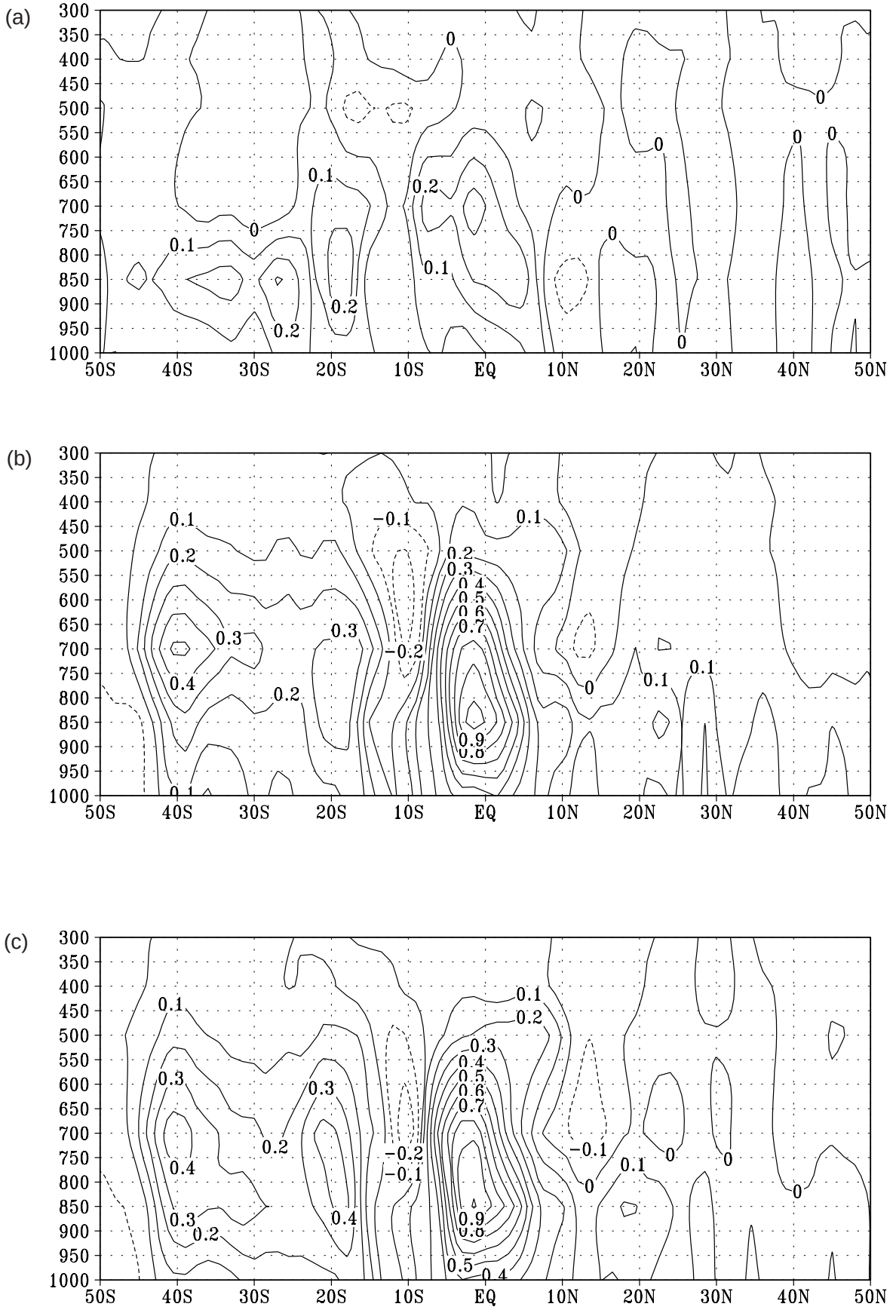

Figure 7. Vertical cross-section of specific humidity (gm/kg), mean of July 1st –15th, 1999: **(a)** Exp. 1 – CNTR, **(b)** Exp. 2 – CNTR and **(c)** Exp. 3 – CNTR.

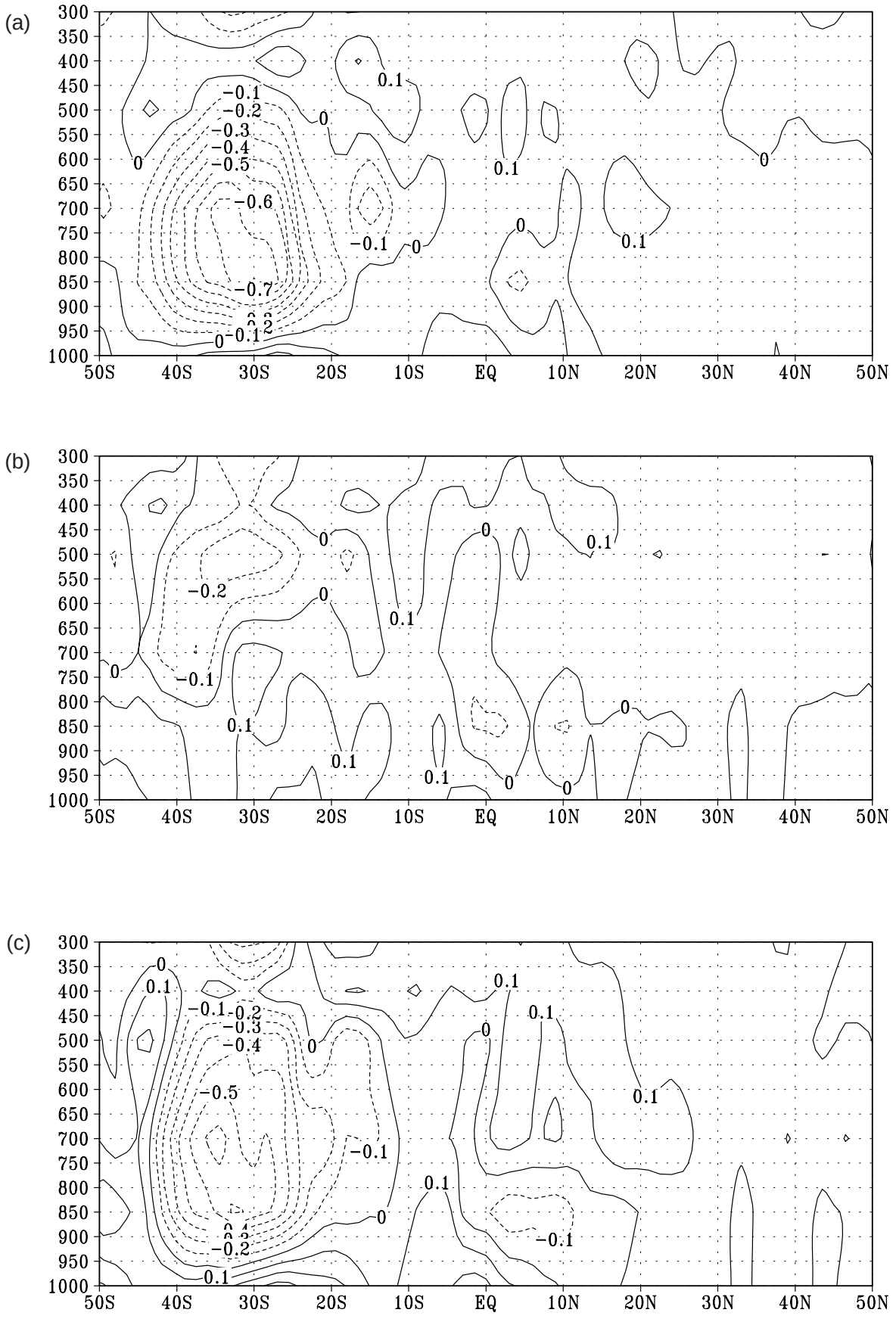

Figure 8. Vertical cross-section of temperature (°K), mean of July 1st –15th, 1999: **(a)** Exp. 1 – CNTR, **(b)** Exp. 2 – CNTR and **(c)** Exp. 3 – CNTR.

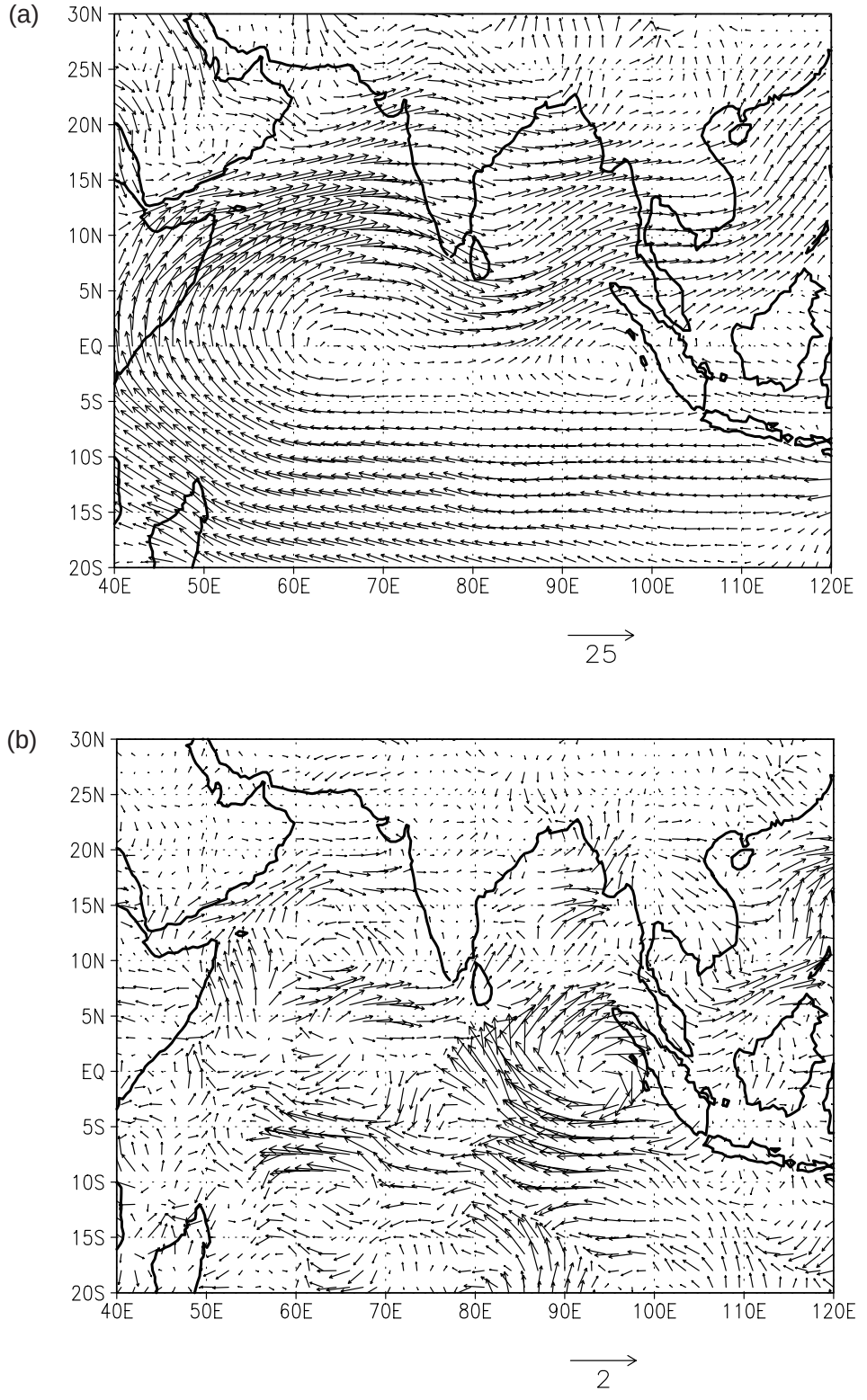

Figure 9. Geographical distribution of mean (July 1st–15th, 1999) **(a)** Wind analysis obtained using 150 km resolution MSMR data and **(b)** difference of wind analyses obtained from 75 km and 150 km resolution MSMR data sets corresponding to Exp. 3.

between experiments using MSMR data and control runs are indicative in nature and rigorous evaluation is required to conclude the usefulness of MSMR data in the NCMRWF data assimilation forecast system. One definite benefit is that the MSMR data are able to remove the dryness of the NCMRWF analyses. However, by utilizing SSM/I data, the same objective is also achieved. Inter-comparison of analyses obtained using SSM/I, MSMR and TRMM (TMI) data will

show the correctness of MSMR results presented in this study.

5. Conclusion

The MSMR data at 75 km resolution from the Oceansat-I have been assimilated in the NCMRWF data assimilation forecast system. The impact of the data is seen globally, however it is significant over the oceanic region where conventional data are rare. The dry-nature of the control analyses have been removed. Therefore, the total precipitable water data from MSMR has been identified as a very crucial parameter in this study. The impact of surface wind speed from MSMR is confined to lower troposphere only, but the TPWC impact is seen at all levels. The impact of surface wind speed from MSMR is to increase easterlies over the tropical Indian Ocean. Shifting of the positions of westerly troughs and ridges in the south Indian Ocean have contributed to reduction of temperature around 30°S. The differences between experiments using MSMR data and control runs are indicative in nature and rigorous evaluation is required to conclude the usefulness of MSMR data in the NCMRWF data assimilation forecast system.

Acknowledgements

The authors are grateful to the Head, NCMRWF for providing all the facilities to carry out this study. MSMR data are provided by SAC, Ahmedabad and NRSA, Hyderabad. This work is partly supported by SAC, ISRO.

References

Chang S W and Holt T R 1994 Impact of assimilating SSM/I rainfall rates on numerical prediction of winter cyclones; *Mon. Weather Rev.* **122** 151–164

Eymard L, Bernard R and Lojou J Y 1993 Validation of microwave radiometer geophysical parameters using meteorological model analysis; *Int. J. Rem. Sens.* **14** 1945–1963

Goswami B N and Rajagopal E N 2002 Comparison of NCMRWF surface winds over the Indian Ocean with *in situ* observations and quick-scat winds. (Manuscript under preparation)

Kanamitsu M 1989 Description of the NMC global data assimilation and forecast system; *Weather Forecasting* **4** 335–342

Ledvina D V and Pfaendtner J 1995 Inclusion of special sensor microwave/ imager (SSM/I total precipitable water content estimates into the GEOS-1 data assimilation system; *Mon. Weather Rev.* **123** 3003–3015

Lorenc A C 1986 Analysis methods for numerical weather prediction; *Quart. J. Roy. Meteor. Soc.* **112** 1177–1194

Parrish D F and Derber J C 1992 The National Meteorological Center's spectral statistical interpolation analysis system; *Mon. Weather Rev.* **120** 1747–1763

Rizvi S R H and Parrish D F 1995 Documentation of the Spectral Statistical Interpolation (SSI) Scheme; *Technical Report. 1/1995, DST*, NCMRWF, New Delhi, India.

Rizvi S R H, Rupa K and Mohanty U C 2000 Report on the utilization of MSMR data in the NCMRWF global data assimilation system; *Report no. 1/2000.* NCMRWF, New Delhi.

Rizvi S R H, Rupa K and Mohanty U C 2002 Impact of MSMR data on NCMRWF Global Data Assimilation System; *Metero. Atmos. Phys.* (accepted)

Schluessel P and Emery W J 1990 Atmospheric water vapour over oceans from SSM/I measurements; *Int. J. Remote Sens.* **11(5)** 753–766

Schluessel P and Luthardt H 1991 Surface wind speeds over the north sea from special sensor microwave/Imager observations; *J. Geophys. Res.* **96(c3)** 4845–4853

Varma A K, Gairola R M, Basu S, Singh K P and Pandey P C 1998 A comparative study of near concurrent DMSP-SSM/I and geosat-altimeter measurements of ocean winds over the Indian oceanic region; *Int. J. Remote Sens.* **19** 717–730

Weng F, Grody N C, Ferraro R, Basisi A and Forsyth D 1997 Cloud liquid water climatology from the special sensor microwave imager; *J. Climate* 1086–1098

Xiao Q, Zou X and Kuo Y H 2000 Incorporating the SSM/I derived precipitable water and rainfall rate into a numerical model : A case study for the ERICA IOP-4 cyclone; *Mon. Weather Rev.* **128** 87–128